

Enhanced torque control for horizontal-axis wind turbines via disturbance observer assistance

Edwin Villarreal-López^{1,2}, Horacio Coral-Enriquez², Sergio Tamayo-León³

¹Departamento de Ingeniería Electrónica, Facultad de Ingeniería, Fundación Universitaria Los Libertadores, Bogotá, Colombia

²Departamento de Ingeniería Mecatrónica, Facultad de Ingeniería, Universidad de San Buenaventura, Bogotá, Colombia

³Department of Flight Dynamics and Control Systems, Institute of Aerospace Engineering, Samara National Research University, Samara, Russia

Article Info

Article history:

Received Jun 13, 2024

Revised Jun 20, 2025

Accepted Aug 1, 2025

Keywords:

Active disturbance rejection control

Disturbance compensation

Energy capture maximization

Extended-state observer

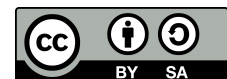
Observer assistance

Wind turbines

ABSTRACT

This paper presents an enhanced control strategy for optimizing energy capture in horizontal axis wind turbines operating in the partial-load region (region 2). The proposed approach builds upon conventional standard torque control (STC) by incorporating a generalized extended state observer (GESO) that follows the active-disturbance-rejection paradigm. Although traditional torque control methods have proven effective under steady wind conditions, they often lack robustness against disturbances, system faults, and model uncertainties inherent in wind energy systems. The proposed observer-assisted control scheme addresses these limitations by estimating and compensating for total disturbance signals, including non-modeled dynamics, parameter uncertainties, and actuator faults. The effectiveness of the proposed control strategy is validated through comprehensive simulations using a 5 MW wind turbine model subjected to realistic operational conditions. Simulation scenarios include turbulent wind speed profiles and actuator degradation to assess controller performance. The results demonstrate improved robustness and energy capture efficiency compared to the conventional control approach, while maintaining the simplicity of the implementation. This work contributes to the development of more reliable wind energy conversion systems (WECSs) by offering a practical solution that improves both performance and fault tolerance in partial load operation.

This is an open access article under the [CC BY-SA](#) license.



Corresponding Author:

Edwin Villarreal-López

Departamento de Ingeniería Electrónica, Facultad de Ingeniería, Fundación Universitaria Los Libertadores

Carrera 16 N° 63A -68, Bogotá, Colombia

Email: evillarreal@libertadores.edu.co

1. INTRODUCTION

Wind energy has become an essential renewable resource in the transition towards clean power generation energy systems [1]. With increasing concerns about climate change and environmental sustainability, optimizing wind turbine performance has become essential for maximizing clean energy generation [2]. Efficient control strategies are critical for wind turbine operation by simultaneously maximizing energy harvesting and reducing mechanical strain through periodic load reduction [3] and minimizing electromechanical wear [4], thereby enhancing both performance and structural longevity [5], [6].

Wind turbine operation is usually divided into three regions considering wind speed conditions [7]. Region 1 for low wind speeds where the turbine is stopped because of lack of enough power compared to

system losses. Region 2 starts from the cut-in to the rated speed, and the control focuses on maximizing the capture of wind energy by modifying the aerodynamic efficiency, which depends on the interaction between the optimal angle of the blade-pitch β_{opt} and the tip speed ratio (TSR), where the power coefficient $C_P(\lambda, \beta)$ is required to remain at its peak value $C_{P_{opt}} = C_P(\lambda_{opt}, \beta_{opt})$. Region 3 deals with wind speeds ranging from rated to cut-off thresholds, where the primary goal is to keep generated power close to its nominal level [8]. In this zone, power capture must be limited to ensure safe operation. The transition region must provide smooth switching between regions 2 and 3 [9].

Various control challenges arise from the highly nonlinear aerodynamics of the rotor, system faults, external disturbances, and model uncertainties. The control method significantly impacts power generation and capture efficiency [10]. This situation motivates the exploration of alternative control concepts to develop more efficient and reliable wind energy conversion systems (WECSs).

Multiple control methods have been introduced to address the issue of maximization of energy harvesting in region 2 [11]. These techniques typically handle wind turbine complexity through linearization or non-linear control methods, each with their advantages and limitations. Standard torque control (STC) [12], [13] or maximum power point tracking [14] has proven effective for steady wind conditions, but lacks robustness against disturbances.

Although observer-based approaches have been proposed [15]–[17], they often introduce significant complexity. This paper proposes a simpler and more versatile strategy using a disturbance observer-based plug-in concept. Following the active-disturbance-rejection (ADR) paradigm [18], [19], we introduce a generalized extended state observer (GESO) that integrates with STC. The GESO estimates total disturbance signals encompassing non-modeled dynamics, parameter uncertainty, faults, and external disturbances, enabling their compensation through the control law.

The following sections are arranged as: section 2 presents the conventional STC approach and its limitations. Section 3 describes the wind turbine model used for controller design. Section 4 introduces the proposed observer-assisted control scheme and its theoretical framework. Section 5 presents simulation results demonstrating the effectiveness of the proposed approach. Finally, conclusion are drawn in section 6.

2. STANDARD TORQUE CONTROL

In region 2, the main control requirement is to maximize power extraction from the wind flow. STC has been widely applied for the operation of wind turbines in this condition [13], [20]. The STC methodology keeps the blade pitch angle at its optimal value β_{opt} while modulating the generator torque according to the rotor angular speed ω_r , following the relationship: $T_{g,ref} = k\omega_r^2$ where k is the optimal controller gain, defined as: $k = 0.5\rho\pi R^5 \frac{C_{p_{max}}}{\lambda_{opt}^3}$.

This approach requires the optimal tip speed ratio λ_{opt} , obtained from the specifications of the wind turbine design, which optimizes the power coefficient $C_{p_{max}}$. However, this control strategy presents several notable drawbacks [21]. First, it requires accurate values of λ_{opt} and $C_{p_{max}}$, parameters that depend on time-varying blade aerodynamics [22]. Furthermore, previous research [13] has shown that alternative expressions for k can increase energy capture under parameter uncertainty when incorporating information on wind turbulence intensity. Furthermore, a fixed k value does not ensure optimal energy capture under real operating conditions, as shown in [23].

This paper formulates a complement for the STC to improve its robustness, based on an extended observer for state and disturbance estimation. The proposed scheme preserves the straightforward implementation of the STC with the robustness provided by disturbance observers.

3. WIND TURBINE MODEL

The use of simulation models for WECS design and control has been widely applied in both academic and industrial environments. Their ability to accurately represent real-world wind turbines has been extensively demonstrated. Many previous works have been conducted in simulation environments, given the complexity, size, high cost, safety concerns, and limited availability of the equipment involved. These factors have motivated the development of models with varying levels of complexity.

Odgaard *et al.* [24] a wind turbine system model used for fault isolation/detection provides a standard platform to evaluate control techniques regarding speed and robustness. However, due to nonlinearities

and challenges in parameter determination, exact analytical representations are unachievable. Hence, higher complexity models with detailed structural and aerodynamic characteristics are continuously developed [25], [26].

Advanced models include Garrad Hassan Bladed (GH-Bladed) from Det Norske Veritas – Germanischer Lloyd (DNV-GL) [27], horizontal axis wind turbine simulation code 2nd generation (HAWC2) from Technical University of Denmark (DTU) wind energy [28], and fatigue, aerodynamics, structures, and turbulence (FAST) from National Renewable Energy Laboratory (NREL) [29], which incorporate aeroelastic properties for fatigue and load analysis. In the context of this work, the nonlinear model given in [24] is employed to validate the developed control strategy.

3.1. Aerodynamic subsystem

Wind-derived rotor energy P_r can be expressed according to (1):

$$P_r = \frac{1}{2} \rho S C_P V_e^3 \quad [W] \quad (1)$$

where ρ denotes density of air, S signifies the rotor's swept area, and V_e represents the relative wind velocity at the rotor, defined later, and C_P is a non-dimensional power coefficient, depending of the wind turbine features, the collective pitch angle of the blades β and the TSR λ ; the relation between wind speed and the linear velocity on the blade tip, which is given by $\lambda = \frac{R\omega_r}{V_e}$, where R is the rotor radius and ω_r is the rotor speed. Rotation torque T_r is produced by interaction between wind flow and blades. However, this also causes a thrust force F_t on the nacelle transmitted to the tower. T_r and F_t are defined as:

$$T_r = \frac{1}{2} \rho S R C_Q V_e^2 \quad [Nm] \quad (2)$$

$$F_T = \frac{1}{2} \rho S R C_T V_e^2 \quad [N] \quad (3)$$

where $C_Q = \frac{C_P}{\lambda}$ represents the torque coefficient and C_T denotes the thrust coefficient, both of which are influenced by the turbine's design characteristics [30].

3.2. Structural dynamics subsystem

The structural dynamics is given by the interaction between tower, blades and drive-train components of the wind turbine. According to [30] this dynamics is written as:

$$(m_t + N m_b) \ddot{y}_t + N m_b r_b \ddot{\xi} + B_t \dot{y}_t + K_t y_t = N F_T \quad (4)$$

$$m_b r_b \ddot{y}_t + m_b r_b^2 \ddot{\xi} + B_b r_b^2 \dot{\xi} + K_b r_b^2 \xi = r_b F_T \quad (5)$$

For the tower, we have the top mass of the tower m_t , damping B_t , stiffness K_t and fore-aft bending displacement y_t . On the other hand, for the N blades, we have the equivalent mass m_b , radius r_b , B_b and K_b damping and stiffness coefficient, respectively, and flapwise angular displacement ξ . Finally, V_w is the absolute wind speed and V_e , the rotor experiences an effective wind speed defined as $V_e = V_w - \dot{y}_t - r_b \dot{\xi}$.

It is possible to describe the drive-train as a two-mass system connected using a flexible shaft coupled with a gear train. The drive-train dynamics can be computed as [31]:

$$J_r \dot{\omega}_r = T_r + \frac{B_{dt}}{N_g} \omega_g - K_{dt} \theta_s - (B_{dt} + B_{ls}) \omega_r \quad (6)$$

$$J_g \dot{\omega}_g = \frac{K_{dt}}{N_g} \theta_s + \frac{B_{dt}}{N_g} \omega_r - \left(\frac{B_{dt}}{N_g^2} + B_{hs} \right) \omega_g - T_g \quad (7)$$

$$\dot{\theta}_s = \omega_r - \frac{1}{N_g} \omega_g \quad (8)$$

where J_r and θ_r are the rotor inertia and angle, B_{dt} , B_{ls} and B_{hs} are damping of the drive-train, low-speed and high-speed shafts, respectively, K_{dt} is the drive-train stiffness, θ_g , ω_g and T_g are the generator angle, speed and torque, and N_g is the gear ratio. The torsion angle of the flexible shaft is $\theta_s = \theta_r - (1/N_g) \theta_g$.

3.3. Pitch and generator subsystems

Considering β_d as the reference angle, pitch subsystem dynamics can be adequately represented as a simplified first order (9), as defined in [30], [31]:

$$\dot{\beta} = -\frac{1}{\tau}\beta + \frac{1}{\tau}\beta_d \quad [rad/s] \quad (9)$$

where τ is the time constant. Generator dynamics is given by [24]:

$$\dot{T}_g = -\frac{1}{\tau_g}T_g + \frac{1}{\tau_g}T_{g,d} \quad [Nm/s] \quad (10)$$

with $T_{g,d}$ is the torque reference; Finally, the produced power of a generator with η_g efficiency is:

$$P_g = \eta_g \omega_g T_g \quad [W] \quad (11)$$

4. IMPROVED STC THROUGH OBSERVER ASSISTANCE

In this section, an ADR observer-assisted STC is proposed. The control scheme builds upon the original STC law but enhances robustness against exogenous and endogenous disturbances. To achieve this, an observer within the ADR framework is introduced to estimate all disturbances affecting the WECS, which are subsequently canceled using a modified version of the STC law.

4.1. Control design

Based on (6)-(8) and (10), the wind turbine and the power converter satisfy the following dynamics:

$$\begin{aligned} \frac{d}{dt}x(t) &= Ax(t) + BT_{g,d}(t) + B\Delta_d(t) + F\omega_r(t) \\ y(t) &= Cx(t) \end{aligned} \quad (12)$$

with,

$$\begin{aligned} x(t) &= \begin{bmatrix} \omega_g(t) \\ \theta_s(t) \\ T_g(t) \end{bmatrix}, \quad A = \begin{bmatrix} -\frac{1}{J_g} \left(\frac{B_{dt}}{N_g^2} + B_{hs} \right) & \frac{K_{dt}}{J_g N_g} & -\frac{1}{J_g} \\ -\frac{1}{N_g} & 0 & 0 \\ 0 & 0 & -\alpha_{gc} \end{bmatrix} \\ B &= \begin{bmatrix} 0 \\ 0 \\ \alpha_{gc} \end{bmatrix}, \quad F = \begin{bmatrix} \frac{B_{dt}}{J_g N_g} \\ 1 \\ 0 \end{bmatrix}, \quad C = \begin{bmatrix} 1 & 0 & 0 \\ 0 & 0 & 1 \end{bmatrix} \end{aligned}$$

where $\alpha_{gc} = 1/\tau_g$, and $\Delta_d(t)$ is an exogenous disturbance function that encompasses all uncertainties associated with the system. These include uncharacterized system behaviors, additive disturbances, actuator malfunctions, parameter drift, and the inherent nonlinear response characteristics of wind turbines. With respect to the dynamic model presented (12), the following assumptions are stated:

- If $\Delta_d(t)$ admits uniformly bounded derivatives of order up to n , for some sufficiently large n , then there exists a constant $K_{\Delta_d} < \infty$, satisfying.

$$\sup_{t \geq 0} |\Delta_d^{(n)}(t)| \leq K_{\Delta_d}$$

- The unmodeled disturbance $\Delta_d(t)$ admits representation through the approximation of its internal structure expressed as:

$$\frac{d^n \Delta_d(t)}{dt^n} \approx 0 \quad (13)$$

Given the disturbance model (13), consider the state-vector of the disturbance signal:

$$x_{\Delta}(t) = \begin{bmatrix} \Delta_d(t) & \dot{\Delta}_d(t) & \cdots & \Delta_d^{(n-2)}(t) & \Delta_d^{(n-1)}(t) \end{bmatrix}^T \quad (14)$$

where the associated dynamical equations are defined by:

$$\begin{aligned} \frac{d}{dt}x_{\Delta}(t) &= A_{\Delta}x_{\Delta}(t) + B_{\Delta}\Delta_d^{(n)}(t) \\ \Delta_d(t) &= C_{\Delta}x_{\Delta}(t) \end{aligned} \quad (15)$$

with,

$$A_{\Delta} = \begin{bmatrix} \mathbf{0}_1 & \mathbf{I}_{n-1} \\ \mathbf{0}_1 & \mathbf{0}_{n-1} \end{bmatrix} \in \mathbb{R}^{n \times n}, \quad B_{\Delta} = \begin{bmatrix} \mathbf{0}_{n-1} \\ 1 \end{bmatrix} \in \mathbb{R}^{n \times 1}, \quad C_{\Delta} = [1 \quad \mathbf{0}_{n-1}] \in \mathbb{R}^{1 \times n}$$

where $x_{\Delta}(t) \in \mathbb{R}^{n \times 1}$. Then, in order to augment the states of the system (12) with the state-vector $x_{\Delta}(t)$ of the disturbance $\Delta_d(t)$; the following formulation is given:

$$\begin{aligned} \frac{d}{dt}x_c(t) &= A_c x_c(t) + B_{c1}T_{g,d}(t) + B_{c2}\omega_r(t) + B_{c3}\Delta_d^{(n)}(t) \\ y(t) &= C_c x_c(t) \end{aligned} \quad (16)$$

with,

$$\begin{aligned} x_c(t) &= \begin{bmatrix} x(t) \\ x_{\Delta}(t) \end{bmatrix} \in \mathbb{R}^{(n+3) \times 1}, \quad A_c = \begin{bmatrix} A & BC_{\Delta} \\ 0 & A_{\Delta} \end{bmatrix} \in \mathbb{R}^{(n+3) \times (n+3)}, \quad B_{c1} = \begin{bmatrix} B \\ 0 \end{bmatrix} \in \mathbb{R}^{(n+3) \times 1} \\ B_{c2} &= \begin{bmatrix} F \\ 0 \end{bmatrix} \in \mathbb{R}^{(n+3) \times 1}, \quad B_{c3} = \begin{bmatrix} 0 \\ B_{\Delta} \end{bmatrix} \in \mathbb{R}^{(n+3) \times 1}, \quad C_c = [C \quad 0] \in \mathbb{R}^{2 \times (n+3)} \end{aligned}$$

Given above assumptions, reconstruction of the disturbance dynamics $\Delta_d(t)$, expressed as $\hat{\Delta}_d(t)$, is provided by the subsequent extended-state observer:

$$\begin{aligned} \frac{d}{dt}\hat{x}_c(t) &= A_c \hat{x}_c(t) + B_{c1}T_{g,d}(t) + B_{c2}\omega_r(t) + L(y(t) - C_c \hat{x}_c(t)) \\ \hat{\Delta}_d(t) &= [0 \quad C_{\Delta}] \hat{x}_c(t) \end{aligned} \quad (17)$$

Let the estimated state vector be defined as $\hat{x}_c(t) = [\hat{\omega}_g(t) \quad \hat{\theta}_s(t) \quad \hat{T}_g(t) \quad \hat{\Delta}_d(t) \quad \hat{\Delta}_d^{(1)}(t) \quad \dots \quad \hat{\Delta}_d^{(n-1)}(t)]^T$, where each component corresponds to an estimated state variable of the system. The matrix L denotes the observer gain, designed such that the eigenvalues of the matrix $[A_c - LC_c]$ lie strictly in the open left-half complex plane, thereby ensuring asymptotic stability of the estimation error dynamics. The observer described by (17) guarantees that the disturbance signal $\Delta_d(t)$ is reconstructed both asymptotically and exponentially. Consequently, the estimation error $\tilde{x}_c(t) = x_c(t) - \hat{x}_c(t)$ converges exponentially to a neighborhood of the origin in the estimation error state space, with the size of this neighborhood determined by the system's disturbance and modeling uncertainties. This eigenvalue placement requirement ensures the asymptotic stability of the observer dynamics and guarantees that estimation errors converge to zero over time.

Given accurate estimations of $\omega_g(t)$ and $\Delta_d(t)$, the applied control law is expressed as:

$$T_{g,d}(t) = k_{opt}\hat{\omega}_g^2(t) - \hat{\Delta}_d(t) \quad (18)$$

where $\hat{\omega}_g(t)$ and $\hat{\Delta}_d(t)$ are supplied through the extended-state observer given before. The proposed control law attenuates disturbances in the WECS and forces the system to behave in nominal conditions.

5. RESULTS

The structure of the ADR observer-assisted STC is shown in Figure 1. From this structure, the disturbance signal $\Delta_d(t)$ is estimated and rejected by the control law. Additionally, the estimated generator speed $\hat{\omega}_g(t)$ is substituted with the measured signal to avoid the effects of sensor noise. This scheme preserves the existing performance characteristics of the conventional controller while improving the robustness of the control system.

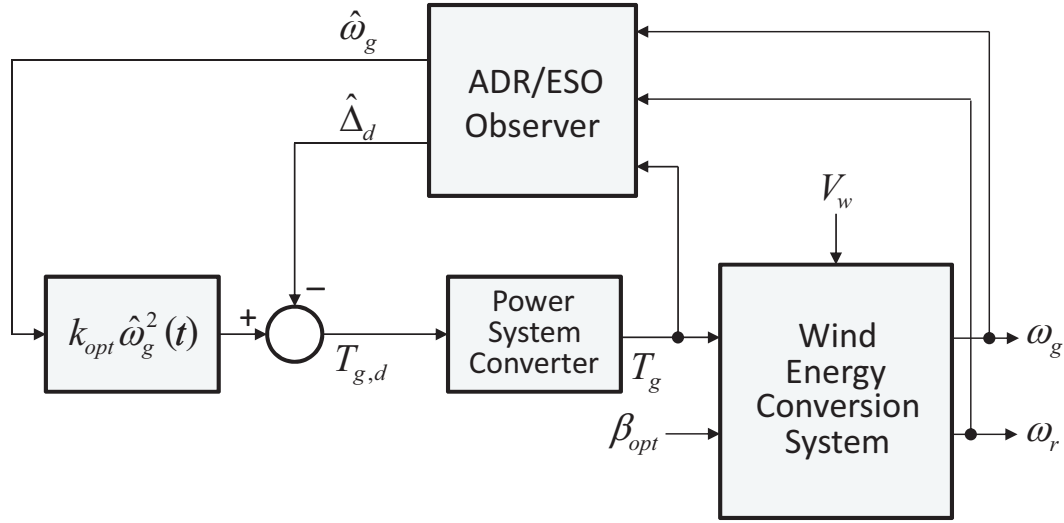


Figure 1. Structural overview of the control loop integrating the observer assisted STC methodology

By defining a first-order internal model ($n = 1$) of the disturbance function $\Delta_d(t)$, the augmented state-space system is given by:

$$\begin{aligned} \frac{d}{dt}x_c(t) &= A_c x_c(t) + B_{c1}T_{g,d}(t) + B_{c2}\omega_r(t) + B_{c3}\dot{\Delta}_d(t) \\ y(t) &= C_c x_c(t) \end{aligned} \quad (19)$$

with,

$$x_c(t) = \begin{bmatrix} \omega_g(t) \\ \theta_s(t) \\ T_g(t) \\ \Delta_d(t) \end{bmatrix}, \quad A_c = \begin{bmatrix} -\frac{1}{J_g} \left(\frac{B_{dt}}{N_g^2} + B_{hs} \right) & \frac{K_{dt}}{J_g N_g} & -\frac{1}{J_g} & 0 \\ -\frac{1}{N_g} & 0 & 0 & 0 \\ 0 & 0 & -\alpha_{gc} & \alpha_{gc} \\ 0 & 0 & 0 & 0 \end{bmatrix}$$

$$B_{c1} = \begin{bmatrix} 0 \\ 0 \\ \alpha_{gc} \\ 0 \end{bmatrix}, \quad B_{c2} = \begin{bmatrix} \frac{B_{dt}}{J_g N_g} \\ 1 \\ 0 \\ 0 \end{bmatrix}, \quad B_{c3} = \begin{bmatrix} 0 \\ 0 \\ 0 \\ 1 \end{bmatrix}, \quad C_c = \begin{bmatrix} 1 & 0 & 0 & 0 \\ 0 & 0 & 1 & 0 \end{bmatrix}$$

Then, the observer is formulated as:

$$\begin{aligned} \frac{d}{dt}\hat{x}_c(t) &= A_c \hat{x}_c(t) + B_{c1}T_{g,d}(t) + B_{c2}\omega_r(t) + L(y(t) - C_c \hat{x}_c(t)) \\ \hat{\Delta}_d(t) &= [0 \ 0 \ 0 \ 1] \hat{x}_c(t) \end{aligned} \quad (20)$$

where, L is the observer gain matrix, chosen in order to provide the following closed-loop eigenvalues $\{-1, -2, -4, -6\}$. In consequence, the control law (18) can be built using the signals $\hat{\omega}_g(t)$ and $\hat{\Delta}_d(t)$ provided by the observer (20).

Figure 2 compares the power capture performance of the proposed ADR Observer-assisted STC approach against conventional STC. While both methods exhibit similar behavior under fault-free conditions, the ADR Observer-assisted STC approach significantly outperforms conventional STC during actuator fault conditions by minimizing energy loss. The proposed method achieves 95.77% aerodynamic efficiency versus 85.87% for standard STC, demonstrating robustness improvements.

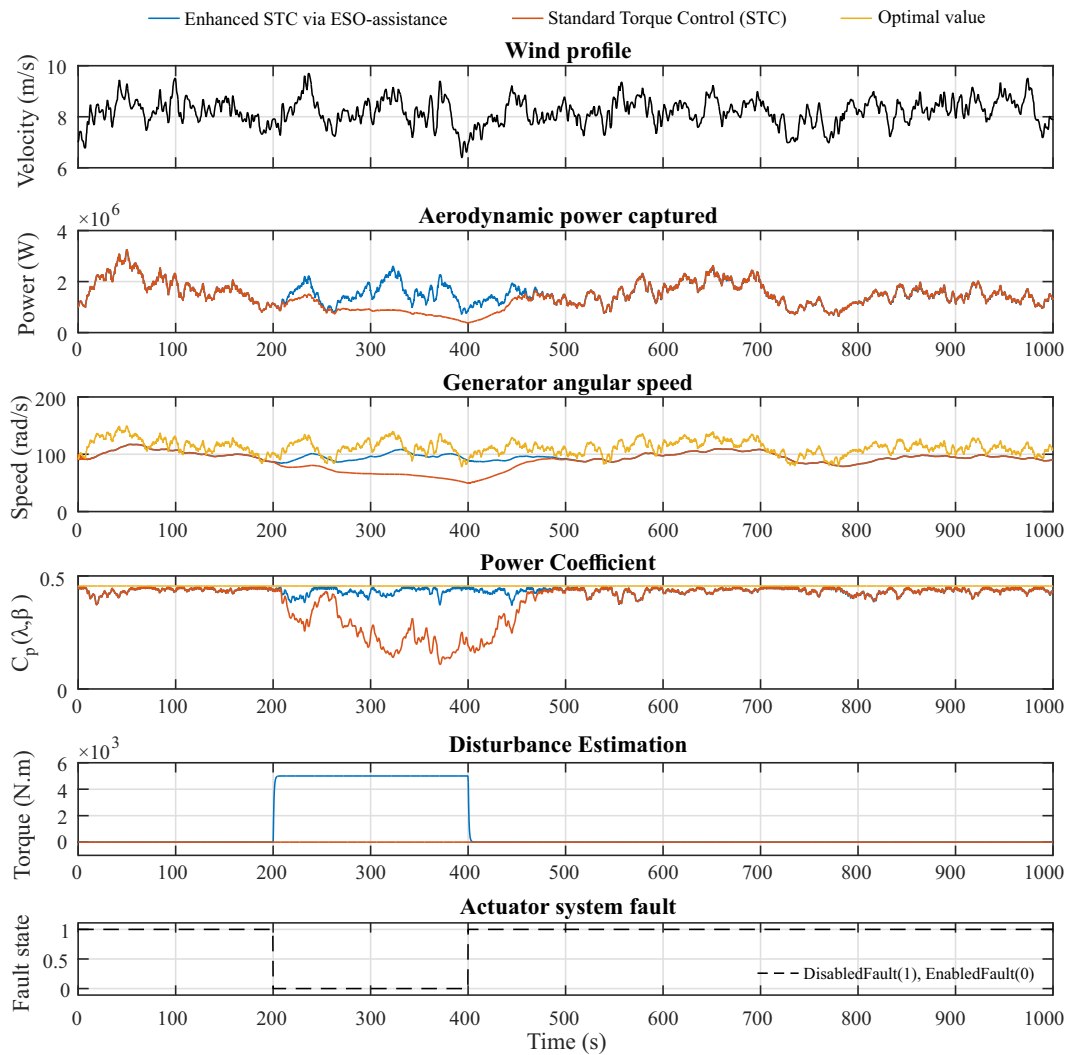


Figure 2. Simulation-based performance evaluation of the enhanced observer-assisted torque control strategy in the presence of fault disturbances applied to the power converter

6. CONCLUSION

This paper presents an enhanced torque control strategy (eSTC) for horizontal axis wind turbines operating in the partial-load region through the integration of a GESO within the ADR framework. The proposed approach successfully addresses the fundamental limitations of conventional STC by providing systematic compensation for model uncertainties and external disturbances, such as actuator faults. The numerical results demonstrate performance improvements, with aerodynamic efficiency under fault conditions, with the increase of energy capture. The plug-in architecture preserves existing STC structure while enhancing system robustness, making the approach viable for practical implementation. Beyond performance benefits, the proposed method contributes to improved system reliability by reducing mechanical stress and potentially extending component lifecycles.

FUNDING INFORMATION

This research was supported by the Universidad de San Buenaventura Bogotá, under research grant FI-019-005, as part of the doctoral research in Engineering of the first author at the Universidad Distrital Francisco José de Caldas.

AUTHOR CONTRIBUTIONS STATEMENT

This journal uses the Contributor Roles Taxonomy (CRediT) to recognize individual author contributions, reduce authorship disputes, and facilitate collaboration.

Name of Author	C	M	So	Va	Fo	I	R	D	O	E	Vi	Su	P	Fu
Edwin Villarreal-López	✓			✓	✓	✓	✓		✓	✓	✓	✓		✓
Horacio Coral-Enriquez	✓	✓			✓				✓	✓		✓	✓	
Sergio Tamayo-León		✓	✓	✓	✓	✓		✓	✓		✓			

C : Conceptualization

M : Methodology

So : Software

Va : Validation

Fo : Formal Analysis

I : Investigation

R : Resources

D : Data Curation

O : Writing - Original Draft

E : Writing - Review & Editing

Vi : Visualization

Su : Supervision

P : Project Administration

Fu : Funding Acquisition

CONFLICT OF INTEREST STATEMENT

Authors state no conflict of interest.

DATA AVAILABILITY

The data that support the findings of this study are available from the corresponding author, E. Villarreal-López, upon reasonable request.




REFERENCES

- [1] Q. Hassan *et al.*, "The renewable energy role in the global energy Transformations," *Renewable Energy Focus*, vol. 48, p. 100545, Mar. 2024, doi: 10.1016/j.ref.2024.100545.
- [2] P. A. Hosseinabadi, H. Pota, S. Mekhilef, and H. Schwartz, "Fixed-time observer-based control of DFIG-based wind energy conversion systems for maximum power extraction," *International Journal of Electrical Power & Energy Systems*, vol. 146, p. 108741, Mar. 2023, doi: 10.1016/j.ijepes.2022.108741.
- [3] A. K. Pamososuryo, S. P. Mulders, R. Ferrari, and J. W. Van Wingerden, "On the Analysis and Synthesis of Wind Turbine Side-Side Tower Load Control via Demodulation," *IEEE Transactions on Control Systems Technology*, vol. 32, no. 5, pp. 1865–1880, Sep. 2024, doi: 10.1109/TCST.2024.3377508.
- [4] A. Aminzadeh *et al.*, "Non-Contact Inspection Methods for Wind Turbine Blade Maintenance: Techno-Economic Review of Techniques for Integration with Industry 4.0," *Journal of Nondestructive Evaluation*, vol. 42, no. 2, p. 54, Jun. 2023, doi: 10.1007/s10921-023-00967-5.
- [5] A. Cadoret, E. D. Goy, J.-M. Leroy, J.-L. Pfister, and L. Mevel, "Linear time periodic system approximation based on Floquet and Fourier transformations for operational modal analysis and damage detection of wind turbine," *Mechanical Systems and Signal Processing*, vol. 212, p. 111157, Apr. 2024, doi: 10.1016/j.ymssp.2024.111157.
- [6] E. J. N. Menezes and A. M. Araújo, "Wind turbine structural control using H-infinity methods," *Engineering Structures*, vol. 286, p. 116095, Jul. 2023, doi: 10.1016/j.engstruct.2023.116095.
- [7] J. Pande, P. Nasikkar, K. Kotecha, and V. Varadarajan, "A Review of Maximum Power Point Tracking Algorithms for Wind Energy Conversion Systems," *Journal of Marine Science and Engineering*, vol. 9, no. 11, p. 1187, Oct. 2021, doi: 10.3390/jmse9111187.
- [8] L. Y. Pao and K. E. Johnson, "A tutorial on the dynamics and control of wind turbines and wind farms," in *2009 American Control Conference, IEEE*, 2009, pp. 2076–2089, doi: 10.1109/ACC.2009.5160195.
- [9] F. Lozano, E. V.-López, and H. C.-Enriquez, "A Bumpless Transfer Control Scheme for Horizontal-Axis Wind Turbines Operating in Transition Region," in *Lecture Notes in Electrical Engineering*, 2021, pp. 501–510, doi: 10.1007/978-3-030-53021-1_51.
- [10] Z. Gao and X. Liu, "An Overview on Fault Diagnosis, Prognosis and Resilient Control for Wind Turbine Systems," *Processes*, vol. 9, no. 2, p. 300, Feb. 2021, doi: 10.3390/pr9020300.
- [11] J. Meyers *et al.*, "Wind farm flow control: prospects and challenges," *Wind Energy Science*, vol. 7, no. 6, pp. 2271–2306, Nov. 2022, doi: 10.5194/wes-7-2271-2022.
- [12] K. Pierce, "Control method for improved energy capture below rated power," *Proceedings of the 1999 3rd ASME/JSME Joint Fluids Engineering Conference, FEDSM'99*, p. 1, 1999.
- [13] K. E. Johnson, L. Y. Pao, M. J. Balas, and J. F. Lee, "Control of Variable-Speed Wind Turbines: Standard and Adaptive Techniques for Maximizing Energy Capture," *IEEE Control Systems*, vol. 26, no. 3, pp. 70–81, Jun. 2006, doi: 10.1109/MCS.2006.1636311.
- [14] W. E. Leithead and B. Connor, "Control of variable speed wind turbines: Design task," *International Journal of Control*, vol. 73, no. 13, pp. 1189–1212, Jan. 2000, doi: 10.1080/002071700417849.
- [15] P. F. Odgaard and J. Stoustrup, "Fault Tolerant Control of Wind Turbines using Unknown Input Observers," *IFAC Proceedings Volumes*, vol. 45, no. 20, pp. 313–318, Jan. 2012, doi: 10.3182/20120829-3-MX-2028.00010.
- [16] H. C.-Enriquez, J. C.-Romero, and G. A. Ramos, "Robust Active Disturbance Rejection Control Approach to Maximize En-



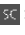
- ergy Capture in Variable-Speed Wind Turbines,” *Mathematical Problems in Engineering*, vol. 2013, pp. 1–12, 2013, doi: 10.1155/2013/396740.
- [17] M. L. Corradini, G. Ippoliti, and G. Orlando, “Fault-tolerant sensorless control of wind turbines achieving efficiency maximization in the presence of electrical faults,” *Journal of the Franklin Institute*, vol. 355, no. 5, pp. 2266–2282, 2018, doi: 10.1016/j.jfranklin.2018.01.003.
- [18] Z. Gao, “Active disturbance rejection control: a paradigm shift in feedback control system design,” in *2006 American Control Conference*, IEEE, 2006, pp. 7 doi: 10.1109/ACC.2006.1656579.
- [19] H. S.-Ramírez, A. L.-Juárez, M. R.-Neria, and E. W. Z.-Bustamante, *Active Disturbance Rejection Control of Dynamic Systems: A Flatness Based Approach*, Butterworth-Heinemann. 2017.
- [20] J. G. Njiri and D. Söffker, “State-of-the-art in wind turbine control: Trends and challenges,” *Renewable and Sustainable Energy Reviews*, vol. 60, pp. 377–393, Jul. 2016, doi: 10.1016/j.rser.2016.01.110.
- [21] E. Iyasere, M. H. Salah, D. M. Dawson, J. R. Wagner, and E. Tatlicioglu, “Robust nonlinear control strategy to maximize energy capture in a variable speed wind turbine with an internal induction generator,” *Journal of Control Theory and Applications*, vol. 10, no. 2, pp. 184–194, 2012, doi: 10.1007/s11768-012-0315-4.
- [22] F. Golnary and H. Moradi, “Dynamic modelling and design of various robust sliding mode controls for the wind turbine with estimation of wind speed,” *Applied Mathematical Modelling*, vol. 65, pp. 566–585, 2019, doi: 10.1016/j.apm.2018.08.030.
- [23] K. E. Johnson, L. J. Fingersh, M. J. Balas, and L. Y. Pao, “Methods for Increasing Region 2 Power Capture on a Variable-Speed Wind Turbine,” *Journal of Solar Energy Engineering*, vol. 126, no. 4, pp. 1092–1100, 2004, doi: 10.1115/1.1792653.
- [24] P. F. Odgaard, J. Stoustrup, and M. Kinnaert, “Fault Tolerant Control of Wind Turbines – a benchmark model,” *IFAC Proceedings Volumes*, vol. 42, no. 8, pp. 155–160, 2009, doi: 10.3182/20090630-4-ES-2003.00026.
- [25] Y. Huang, X. Yang, W. Zhao, and D. Wan, “Aeroelastic analysis of wind turbine under diverse inflow conditions,” *Ocean Engineering*, vol. 307, p. 118235, 2024, doi: 10.1016/j.oceaneng.2024.118235.
- [26] G. D. Posta, S. Leonardi, and M. Bernardini, “A two-way coupling method for the study of aeroelastic effects in large wind turbines,” *Renewable Energy*, vol. 190, pp. 971–992, May 2022, doi: 10.1016/j.renene.2022.03.158.
- [27] DNVGL, “A design tool for wind turbine performance and loading,” <https://www.dnvgl.com/services/bladed-3775>
- [28] J. P. Murcia et al., “Uncertainty propagation through an aeroelastic wind turbine model using polynomial surrogates,” *Renewable Energy*, vol. 119, pp. 910–922, Apr. 2018, doi: 10.1016/j.renene.2017.07.070.
- [29] J. Jonkman, “FAST — NWTC Information Portal,” <https://nwtc.nrel.gov/FAST> (accessed Apr. 01, 2016).
- [30] F. A. Shirazi, K. M. Grigoriadis, and D. Viassolo, “Wind turbine integrated structural and LPV control design for improved closed-loop performance,” *International Journal of Control*, vol. 85, no. 8, pp. 1178–1196, Aug. 2012, doi: 10.1080/00207179.2012.679973.
- [31] C. Sloth, T. Eshensen, and J. Stoustrup, “Robust and fault-tolerant linear parameter-varying control of wind turbines,” *Mechatronics*, vol. 21, no. 4, pp. 645–659, Jun. 2011, doi: 10.1016/j.mechatronics.2011.02.001.

BIOGRAPHIES OF AUTHORS






Edwin Villarreal-López    received the B.Eng. degree in Design and Electronics Automation Engineering from the Universidad de La Salle, Bogotá, Colombia, in 2004, and the Master's degree in Industrial Automation Engineering from the Universidad Nacional de Colombia, Bogotá, Colombia, in 2008. He is currently pursuing a Ph.D. degree with the Faculty of Engineering at the Universidad Distrital Francisco José de Caldas. He is a Research Associate Professor of the Faculty of Engineering at the Universidad de San Buenaventura, Bogotá, Colombia. His current research interest include fault detection and isolation, active disturbance rejection control, and applications of control theory. He can be contacted at email: evillarreal@libertadores.edu.co.



Horacio Coral-Enriquez    received the B.Sc. degree in Engineering in Industrial Automática from the Universidad del Cauca, Popayán, Colombia, in 2005, and the M.Sc. degree in Automática from the Universidad del Valle, Cali, Colombia, in 2010. In 2017 he received the Ph.D. degree (Cum laude) from the Universidad Nacional de Colombia. Currently, he is a Research Associate Professor of the Faculty of Engineering at the Universidad de San Buenaventura, Bogotá, Colombia. He is the author of over 40 technical papers in journals and international conference proceedings. His main research areas include active disturbance rejection control, nonlinear control, wind turbine control, and applications of control theory. He can be contacted at email: hcoral@usbbog.edu.co.



Sergio Tamayo-León    received his B.Sc. degree in Mechatronics Engineering at the San Buenaventura University, Bogotá, Colombia, in 2017. He has published over 4 refereed journal, and conference papers. Currently he is a Master's student at Samara National Research University, in Russia. His main research areas include vehicle dynamics, control theory, artificial gravity, modeling, and control of mechatronic systems. He can be contacted at email: sergioa.tamayo@gmail.com.